Dynamic Load Vectors for Localization of Mass and Stiffness Perturbations

Martin D. Ulriksen*

Department of Energy Technology, Aalborg University, 6700 Esbjerg, Denmark

Abstract

The well-established Dynamic Damage Locating Vector (DDLV) method offers localization of structural damage through a linear transformation of the null vectors of the transfer matrix change or, in the stochastic case of unknown input, a surrogate hereof. The null vectors are referred to as DDLVs, and it has been previously shown how applying these as loads to the structural domain will result in zero steady-state strain in any subdomain containing stiffness perturbations. The present paper explores the use of DDLVs for localization of mass-related damage and proves that any mass perturbation will, upon application of the DDLVs, be confined to the subdomain exhibiting zero steady-state motion. Since the strain field is realized from a surjective linear transformation of the displacement field, the DDLVs allow for localization of both mass- and stiffness-related damage without adding computational complexity to the existing procedures. The paper outlines the interrogation scheme for both damage types and demonstrates the basic principles through numerical and experimental examples.

Keywords: damage localization, dynamic damage locating vectors, mass and stiffness perturbations, structural health monitoring.

1. Introduction

Structural damage localization can be resolved in a setting where damage-induced changes in some set of vibration features are mapped to the structural domain by aid of a model of the undamaged/reference structure [1, 2]. When referring strictly to localization—and not general diagnosis as obtained through, for example, model updating [3, 4, 5]—one of the first examples of a model-based approach is the Best Achievable Eigenvector (BAE) method by Lim and Kashangaki [6]. The premise of the BAE method is to interrogate one element at a time in the model and announce damage when the span of a subspace that depends on the element being considered contains the identified eigenvectors. A requirement here is, as is the case for many of the early model-based localization schemes [2], that the experimental feature is available at all the model coordinates/degrees of freedom (DOF). This requirement will never be satisfied in practice, so the missing experimental entries must be estimated through a coordinate expansion procedure, which often degrades the localization performance severely.

During the last couple of decades, a vast amount of model-based localization methods have been proposed to cope with the issue of matching experimental and model coordinates [7, 8, 9, 10, 11]. A technique that does not rely on the coordinate match is the Damage Locating Vector (DLV) series by Bernal [12, 13, 14, 15]. The Dynamic Damage Locating Vector (DDLV) method [14] is based on a theorem stating that the null vectors of the transfer matrix change due to stiffness perturbations are dynamic loads inducing zero steady-state strain in the perturbed/damaged subdomain. The stochastic DDLV (SDDLV) method extends to cases where the transfer matrices cannot be computed explicitly because the input is unknown. For this prevailing situation, it is shown by Bernal [15] how null vectors of the transfer matrix change due to stiffness perturbations can be extracted from the null space of a matrix that can be estimated from output-only system realizations.

The DDLV and SDDLV methods have demonstrated merit in different laboratory and industrial application studies; including localization of an emulated edge debonding in a residential-sized wind turbine blade [16] and a crack in an onshore wind turbine in idle condition [17]. To increase the robustness of the methods, extensions have been proposed to take into account the statistical uncertainties associated with the embedded output-only realizations from subspace identification [18, 19, 20]. The methodological premise is to estimate the uncertainties using well-established techniques [21] and subsequently propagate them to the strain/stress estimates using the delta method [22]. The net robustness gain obtained by this propagation technique is exemplified by Marin et al. [18] in the context of a laboratory experiment with a cantilevered beam.

*Email: mdu@et.aau.dk.

In the literature, the DDLV and SDDLV methods are presented as means to locate stiffness perturbations. The focus of the present paper is to bring attention to the fact that the methods also allow for localization of mass perturbations, which is of practical interest in, for example, offshore applications where marine growth and ice accretion can alter the mass substantially. It will be shown in Section 2 how application of DDLVs as loads to the structural domain in its reference state will confine potential mass perturbations to the structural subdomain exhibiting zero steady-state motion. In this way, mass perturbations can be located directly from the resulting steady-state displacement fields, while the stiffness perturbations follow from an interrogation of the steady-state strain fields. Since these strain fields are computed through a linear transformation of the displacement fields, the original DDLV and SDDLV methods enable localization of both mass and stiffness perturbations without requiring any methodological extensions.

For stochastic systems, it may appear that the DDLVs, which in this instance are extracted from the null space of a surrogate of the damage-induced transfer matrix change, hinge on the assumption of a perturbation-invariant direct transmission term [15, 18, 19]. Since the direct transmission term depends on the mass (but not the stiffness) of the structural system, such a constraint would invalidate the procedure for localization of mass perturbations in stochastic systems. It will, however, be proved in Section 3 that direct transmission invariance is not a requirement for the null space of the aforementioned surrogate to contain DDLVs. As such, mass perturbations can also be located by use of DDLVs in structural systems that are monitored in an output-only setting.

The main body of the paper is organized as follows. In Section 2, the DDLV method is outlined and a theorem is presented that generalizes the original DDLV theorem by Bernal [14] to take into account mass perturbations as well. The concept is extended to the stochastic situation in Section 3, while Section 4 contains a brief summary of how the schemes are implemented. Numerical examples with a finite element truss structure model and an experimental study with a frame structure follow in Sections 5 and 6, and the paper closes with concluding remarks in Section 7.

2. Deterministic load vectors for localization of mass and stiffness perturbations

A structural system is referred to as *deterministic* when both the input and output are known. In this situation, the DDLVs are—as is shown by Bernal [14] for stiffness perturbations and will be shown in Subsection 2.2 for both mass and stiffness perturbations—extracted directly from the null space of the damage-induced shift in transfer matrix.

2.1. Modeling of deterministic structural systems

We consider a structural domain, Ω, and assume that it, in its reference state, can be described by the linear, time-invariant (LTI) model

$$M\ddot{x}(t) + C\dot{x}(t) + Kx(t) = B_2 u(t), \tag{1}$$

where $\ddot{x}(t)$, $\dot{x}(t)$, $x(t) \in \mathbb{R}^n$ denote the acceleration, velocity, and displacement vectors, $u(t) \in \mathbb{R}^r$ collects the independent inputs that are distributed to Ω by $B_2 \in \mathbb{R}^{n\times r}$, and M, C, $K \in \mathbb{R}^{n\times n}$ are the mass, damping, and stiffness matrices.

System (1) can be rewritten into an N'th order state-space formulation by defining the state vector $z(t) \in \mathbb{R}^N$ and the output vector $y(t) \in \mathbb{R}^m$. Hereby, the continuous-time state-space formulation becomes

$$\dot{z}(t) = A_c z(t) + B_c u(t) \tag{2a}$$

$$y(t) = C_c z(t) + D_c u(t) \tag{2b}$$

where $A_c \in \mathbb{R}^{N\times N}$, $B_c \in \mathbb{R}^{N\times r}$, $C_c \in \mathbb{R}^{m\times N}$, and $D_c \in \mathbb{R}^{m\times r}$ are the state, input, output, and direct transmission matrices. It is noted that in case all the modes of system (1) are identified, then $N = 2n$ and $z(t) = [x(t)^T \ \dot{x}(t)^T]^T$. This will, however, seldom be feasible in practice where the typical scenario is to have a modally truncated approximation with $N \ll 2n$.

The receptance transfer matrix of system (2) is given as [14]

$$G(s) = C_c A_c^{-b} (sI - A_c)^{-1} B_c \tag{3}$$

for $b = 0, 1, 2$ depending on whether the output consists of displacements, velocities, or accelerations. The receptance transfer matrix maps the r inputs to m displacement outputs. We collect the *coordinates* of the r inputs in the set $\mathcal{R}$ and the *coordinates* of the m outputs in the set $\mathcal{M}$. From reciprocity, it follows that if $\mathcal{R} \cap \mathcal{M} \neq \emptyset$ and $q = \#\{\mathcal{R} \cup \mathcal{M}\}$, then the input-output map is $\mathbb{C}^q \to \mathbb{C}^q$. In the derivations made in the present section (the deterministic situation), it will be assumed that this collocated set exists such $G(s) = G(s)^T \in \mathbb{C}^{q\times q}$.

2.2. Extracting the DDLVs

We now consider the situation where the structural domain Ω is analyzed in its reference state and in a damaged state with mass and stiffness perturbations in $\Omega_2 \subset \Omega$. As will be evidenced in Subsection 2.3, Ω_2 does not need to be simply connected.

Definition 1. *$\Omega = \Omega_1 \cup \Omega_2$ is a structural domain with $\Omega_2 = \Omega_2^{\delta K} \cup \Omega_2^{\delta M}$, where $\Omega_2^{\delta K}$ contains any stiffness perturbation δK and $\Omega_2^{\delta M}$ any mass perturbation δM. Thus, in the reference state, $\Omega_2 = \emptyset \Leftrightarrow \Omega = \Omega_1$.*

Definition 2. *Let $G(s)$ and $\tilde{G}(s)$ denote the transfer matrices of Ω in its reference and damaged states and define $\delta G(s) = \tilde{G}(s) - G(s) \in \mathbb{C}^{q\times q}$. Then, $v(s) \in \mathbb{C}^q$ is a DDLV if $0 \neq v(s) \in Null\,(\delta G(s))$.*

Remark 1. *A physical interpretation follows from Definition 2: since $\delta G(s)v(s) = \tilde{G}(s)v(s) - G(s)v(s) = 0$, the DDLVs are loads that enforce identical state-steady response of Ω in its reference and damaged states.*

With $\text{Null}\,(\delta G(s)) \in \mathbb{C}^{q\times(q-p)}$, where $p = \text{Rank}\,(\delta G(s))$, a necessary constraint for the existence of $v(s)$ is obviously that $p < q$. Lemma 1 specifies this constraint in terms of the introduced damage.

Lemma 1. *Let $\delta G(s)$ be given by Definition 2 with perturbations δK and δM, then $p = Rank\,(\delta G(s)) < q$ if $Rank\,(\delta M) + Rank\,(\delta K) < q$.*

Proof. The proof follows as an extension of that by Bernal [14] and explicit reference to the Laplace variable is skipped for notational convenience. The transfer matrix in the damaged state is defined by

$$\tilde{G} = G + \delta G, \tag{4}$$

where $G \in \mathbb{C}^{q\times q}$ is the reference-state transfer matrix (3). Assuming that G and $\tilde{G}$ have full rank, we can write

$$\tilde{G}^{-1} = G^{-1} + \delta M s^2 + \delta K, \tag{5}$$

thus with $X = \delta M s^2 + \delta K$,

$$\tilde{G} = \left(G^{-1} + X\right)^{-1}. \tag{6}$$

The Woodbury matrix identity [23] provides

$$\tilde{G} = G - GX\,(I + GX)^{-1}\,G \tag{7}$$

such

$$\delta G = -GX\,(I + GX)^{-1}\,G, \tag{8}$$

and it is seen that

$$\text{Rank}\,(\delta G) = p \leq \min\left\{\text{Rank}\,(G)\,, \text{Rank}\,(X)\,, \text{Rank}\left((I + GX)^{-1}\right)\right\}. \tag{9}$$

By substituting $X = \delta M s^2 + \delta K$, it follows

$$p \leq \text{Rank}\left(\delta M s^2 + \delta K\right) \leq \text{Rank}\,(\delta M) + \text{Rank}\,(\delta K)\,, \tag{10}$$

hence leading to the constraint $q > \text{Rank}\,(\delta M) + \text{Rank}\,(\delta K)$. □

2.3. Damage localization

The original DDLV theorem by Bernal [14] states that if $\delta G(s)$ is solely governed by δK, then the steady-state strains in Ω_2 will be zero when applying $v(s)$ as a load to Ω. In practice, this is realized by applying $v(s)$ to the *model* transfer matrix of system (1),

$$\mathcal{G}(s) = \left(Ms^2 + Cs + K\right)^{-1}, \tag{11}$$

and computing the steady-state displacements

$$x(s) = \mathcal{G}(s)\mathcal{B}_2 v(s) \tag{12}$$

from which the steady-state strains (one component per element in the model) are obtained as

$$\epsilon(s) = \mathcal{L}_\epsilon x(s). \tag{13}$$

We note that $\mathcal{B}_2 \in \mathbb{R}^{n\times q}$ distributes $v(s)$ to the structural domain, while $\mathcal{L}_\epsilon \in \mathbb{C}^{n_e\times n}$ maps the displacements to one strain component for each of the n_e elements in the model. We now extend the DDLV theorem to also consider mass perturbations.

Theorem 1. *Let Ω be given by Definition 1 and assume that δK and δM induce the transfer matrix shift $\delta G(s) \in \mathbb{C}^{q\times q}$ for which $0 \neq v(s) \in Null\,(\delta G(s))$. Then,* (12) *and* (13) *yield $x_{\Omega_2^{\delta M}} \equiv 0$ and $\epsilon_{\Omega_2^{\delta K}} \equiv 0$.*

Proof. The proof follows under the assumption of $q > \mathrm{Rank}\,(\delta M) + \mathrm{Rank}\,(\delta K)$, as developed in Lemma 1.

(i) Localization of δK: The proof has been provided by Bernal [14], but a summary is included here for clarity. Remark 1 implies that both the steady-state strains and associated strain energy in Ω must be identical in the reference and damaged states, thus

$$\int\limits_{\Omega\backslash\{\Omega_2^{\delta K}\}} \epsilon^T E\epsilon\, dV + \int\limits_{\Omega_2^{\delta K}} \epsilon^T \tilde{E}\epsilon\, dV = \int\limits_{\Omega\backslash\{\Omega_2^{\delta K}\}} \epsilon^T E\epsilon\, dV + \int\limits_{\Omega_2^{\delta K}} \epsilon^T E\epsilon\, dV, \tag{14}$$

where E, $\tilde{E}$ are the constitutive matrices that map strains to stresses in the two structural states. It follows

$$\int\limits_{\Omega_2^{\delta K}} \epsilon^T \tilde{E}\epsilon\, dV = \int\limits_{\Omega_2^{\delta K}} \epsilon^T E\epsilon\, dV, \tag{15}$$

hence leading to the assertion $\epsilon_{\Omega_2^{\delta K}} \equiv 0$ since $E, \tilde{E} \succ 0$ and $\tilde{E} \neq E$.

(ii) Localization of δM: Remark 1 implies that the steady-state motion in Ω must be identical in the reference and damaged states. The same holds for the associated kinetic energy, so when it is assumed, for simplicity but without loss of generality, that δM affects the density, $\rho \in \mathbb{R}_{>0}$, then

$$\int\limits_{\Omega\backslash\{\Omega_2^{\delta M}\}} \rho\dot{x}^T \dot{x}\, dV + \int\limits_{\Omega_2^{\delta M}} \tilde{\rho}\dot{x}^T \dot{x}\, dV = \int\limits_{\Omega\backslash\{\Omega_2^{\delta M}\}} \rho\dot{x}^T \dot{x}\, dV + \int\limits_{\Omega_2^{\delta M}} \rho\dot{x}^T \dot{x}\, dV \tag{16}$$

from which

$$\int\limits_{\Omega_2^{\delta M}} \tilde{\rho}\dot{x}^T \dot{x}\, dV = \int\limits_{\Omega_2^{\delta M}} \rho\dot{x}^T \dot{x}\, dV, \tag{17}$$

so $\dot{x}_{\Omega_2^{\delta M}} \equiv x_{\Omega_2^{\delta M}} \equiv 0$. □

3. Stochastic load vectors for localization of mass and stiffness perturbations

A structural system is referred to as *stochastic* when only the output is known. In this situation, the DDLVs are—as is shown by Bernal [15] for stiffness perturbations and will be shown in Subsection 3.2 for both stiffness and mass perturbations—extracted from the null space of a surrogate of the damage-induced transfer matrix change. When the DDLVs have been extracted from output-only realizations, the localization procedure outlined in Subsection 2.3 applies.

3.1. Modeling of stochastic structural systems

The external force in system (1) is unmeasured but assumed to be white noise. In this instance, $u(t)$ will be replaced by a set of fictive inputs that are collocated with the m outputs such $B_c \in \mathbb{R}^{N\times m}$ and $D_c \in \mathbb{R}^{m\times m}$. We follow the procedure outlined by Bernal [15] and define

$$G(s) = Z(s)B_c \tag{18}$$

with $Z(s) = C_c A_c^{-b}(sI - A_c)^{-1} \in \mathbb{C}^{m\times N}$. The unknown B_c can be expressed as a function of the direct transmission matrix, $D_c = C_c A_c^{1-b} B_c$, which, of course, is also unknown but is used in the following developments. We have [15]

$$B_c = H^\dagger L D_c, \tag{19}$$

where superscript † denotes the Moore-Penrose pseudo-inverse and

$$H = \begin{bmatrix} C_c A_c^{1-b} \\ C_c A_c^{-b} \end{bmatrix} \in \mathbb{R}^{2m\times N}, \quad L = \begin{bmatrix} I \\ 0 \end{bmatrix} \in \mathbb{R}^{2m\times m}, \tag{20}$$

with the constraint $2m \geq N$ to ensure that (19) is a unique solution. Plugging (19) into (18) and defining

$$R(s) = Z(s)H^\dagger L \tag{21}$$

provide

$$G(s) = R(s)D_c, \tag{22}$$

which, due to symmetry in the prescribed collocated set, can be written as

$$G(s) = D_c R(s)^T. \tag{23}$$

For subsequent developments, we now examine the expression $D_c = C_c A_c^{1-b} B_c$. Let M_E, C_E, K_E be the mass, damping, and stiffness matrices in the identified system and $\hat{C}$ the matrix that maps the displacement, velocity, or acceleration vector in (1) to the measured output, $y(t)$. For accelerations ($b = 2$), we get the direct transmission

$$\begin{aligned} D_c &= \begin{bmatrix} -\hat{C}M_E^{-1}K_E & -\hat{C}M_E^{-1}C_E \end{bmatrix} \begin{bmatrix} 0 & I \\ -M_E^{-1}K_E & -M_E^{-1}C_E \end{bmatrix}^{-1} \begin{bmatrix} 0 \\ M_E^{-1}\hat{C}^T \end{bmatrix} \\ &= \begin{bmatrix} -\hat{C}M_E^{-1}K_E & -\hat{C}M_E^{-1}C_E \end{bmatrix} \begin{bmatrix} 0 & 0 \\ 0 & -C_E^{-1}M_E \end{bmatrix} \begin{bmatrix} 0 \\ M_E^{-1}\hat{C}^T \end{bmatrix} = \hat{C}M_E^{-1}\hat{C}^T, \end{aligned} \tag{24}$$

which is readily found to hold for displacement and velocity measurements ($b = 0, 1$) as well.

3.2. Extracting the DDLVs

From the outset of (23), the damage-induced transfer matrix shift can be expressed by

$$\delta G(s) = \tilde{D}_c \tilde{R}(s)^T - D_c R(s)^T \tag{25}$$

or, when defining $\delta R(s) = \tilde{R}(s) - R(s)$ and $\delta D_c = \tilde{D}_c - D_c$,

$$\delta G(s) = \begin{bmatrix} \tilde{D}_c & \delta D_c \end{bmatrix} \begin{bmatrix} \delta R(s)^T \\ R(s)^T \end{bmatrix}. \tag{26}$$

The literature has explored the situation where $\delta M = 0$ and $\delta D_c = 0$ [15, 18, 19]. With these assumptions, it follows that if $v(s) \in \mathrm{Null}(\delta R(s)^T)$, then $v(s) \in \mathrm{Null}(\delta G(s))$. We now examine the situation where $\delta M \neq 0$ such $\delta D_c \neq 0$ and prove that $0 \neq v(s) \in \mathrm{Null}(\delta R(s)^T)$ is still a sufficient constraint for $v(s)$ to be a DDLV.

Theorem 2. *Let $\delta G(s)$ be given by* (26)*, then $v(s)$ is a DDLV if $0 \neq v(s) \in Null(\delta R(s)^T)$.*

Proof. According to Definition 2, $v(s)$ is a DDLV if $0 \neq v(s) \in \mathrm{Null}(\delta G(s))$. With the final result in (24) being valid for homogeneous displacement, velocity, and acceleration measurements, it follows from (23) that

$$R(s)^T = (\hat{C}M_E^{-1}\hat{C}^T)^{-1}G(s). \tag{27}$$

Let $0 \neq v(s) \in \mathrm{Null}(\delta R(s)^T)$ such

$$(\hat{C}\tilde{M}_E^{-1}\hat{C}^T)^{-1}\tilde{G}(s)v(s) - (\hat{C}M_E^{-1}\hat{C}^T)^{-1}G(s)v(s) = 0, \tag{28}$$

so if we, for notational convenience but without loss of generality, assume that $\hat{C} = I$ and $M_E = M$ with M being the mass matrix in system (1), then

$$\tilde{M}\tilde{G}(s)v(s) - MG(s)v(s) = 0. \tag{29}$$

Pre-multiplying with M^{-1} and plugging in $\tilde{M} = M + \delta M$ with

$$\delta M = \begin{bmatrix} 0 & 0 \\ 0 & \delta M_{\Omega_2^{\delta M}} \end{bmatrix} \tag{30}$$

yield

$$(I + M^{-1}\delta M)\tilde{G}(s)v(s) - G(s)v(s) = 0 \Leftrightarrow \delta G(s)v(s) = -M^{-1}\delta M\tilde{G}(s)v(s), \tag{31}$$

which can only hold if $v(s) \in \mathrm{Null}(\delta G(s))$ such $\delta G(s)v(s) = -M^{-1}\delta M\tilde{G}(s)v(s) = 0$. That $M^{-1}\delta M\tilde{G}(s)v(s) = 0$ for $v(s) \in \mathrm{Null}(\delta G(s))$ and δM given by (30) follows from Theorem 1, as $M^{-1}\delta M\tilde{G}(s)v(s) = M^{-1}\delta M[x_{\Omega\setminus\{\Omega_2^{\delta M}\}}(s)^T \;\; 0^T]^T = 0$. □

4. Implementation strategy

Sections 2 and 3 outline how DDLVs can be used to locate mass and stiffness perturbations in both deterministic and stochastic systems. Since no modifications of the original DDLV and SDDLV formulations are required, the schemes can be implemented directly as outlined by Bernal [14, 15] and, optionally, with propagation of uncertainties as proposed by Döhler et al. [18] and Marin et al. [19]. In the present paper, the latter is omitted for conciseness. A summary of the DDLV and SDDLV schemes for simultaneous localization of mass and stiffness perturbations is provided below. For more details on each step, the reader is referred to [14, 15].

1. Estimate $\{A_c, B_c, C_c, D_c\}$ (DDLV) or $\{A_c, C_c\}$ (SDDLV) from the reference and damaged states [24]. Note that consistency in the identified modes is required, thus modes only identified in one of the two states must be discarded.
2. Select a set of n_s s-values at which the interrogation is conducted. To avoid undue truncation errors, the s-values must be in the vicinity of the identified eigenvalues.
3. For each s-value:
   (a) Compute $\delta G(s_j)$ (DDLV) or $\delta R(s_j)^T$ (SDDLV).
   (b) Take $v(s_j)$ as the right singular vector associated with the lowest singular value of $\delta G(s_j)$ or $\delta R(s_j)^T$.
   (c) Compute $x(s_j)$ using (12).
   (d) Compute $\epsilon(s_j)$ using (13).
4. Calculate $\mathcal{X} = \frac{1}{n_s}\sum_{j=1}^{n_s} \frac{|x(s_j)|}{\max|x(s_j)|}$.
5. Calculate $\mathcal{E} = \frac{1}{n_s}\sum_{j=1}^{n_s} \frac{|\epsilon(s_j)|}{\max|\epsilon(s_j)|}$.
6. The entries in $\mathcal{X}$ that are close to zero point to mass-related damage (node- or DOF-wise).
7. The entries in $\mathcal{E}$ that are close to zero point to stiffness-related damage (element-wise).

5. Numerical examples

To exemplify the points made in the previous sections, we examine the finite element truss model depicted in Fig. 1. The truss, which consists of 21 bars that are assigned identical cross-sections and material models, has a first undamped eigenfrequency of 10 rad/s in the reference state. The damping matrix, which is kept fixed in the two structural states, is formed by assuming a classical distribution with 2 % critical damping in each mode in the reference state. In Subsection 5.1, results are presented for simultaneous localization of mass and stiffness perturbations in an idealized setting where noise, modal truncation, and model errors are omitted. Subsection 5.2 outlines localization of a mass perturbation in a stochastic simulation configuration with model errors, noise-contaminated output, and modally truncated approximations of the system matrices.

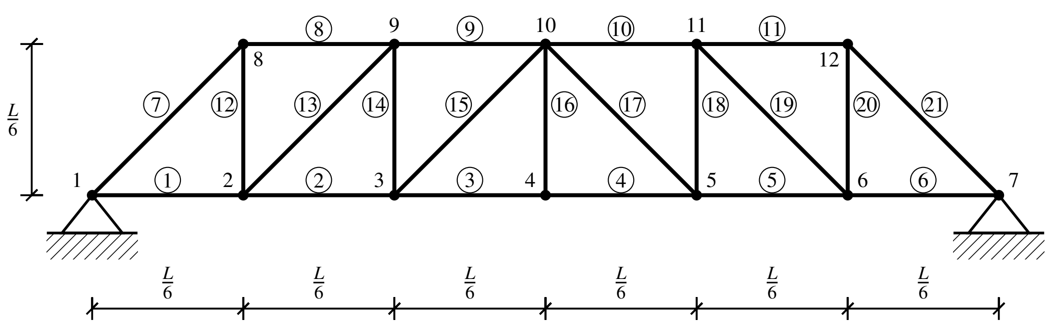

Fig. 1: Finite element truss structure model with node and element numbering.

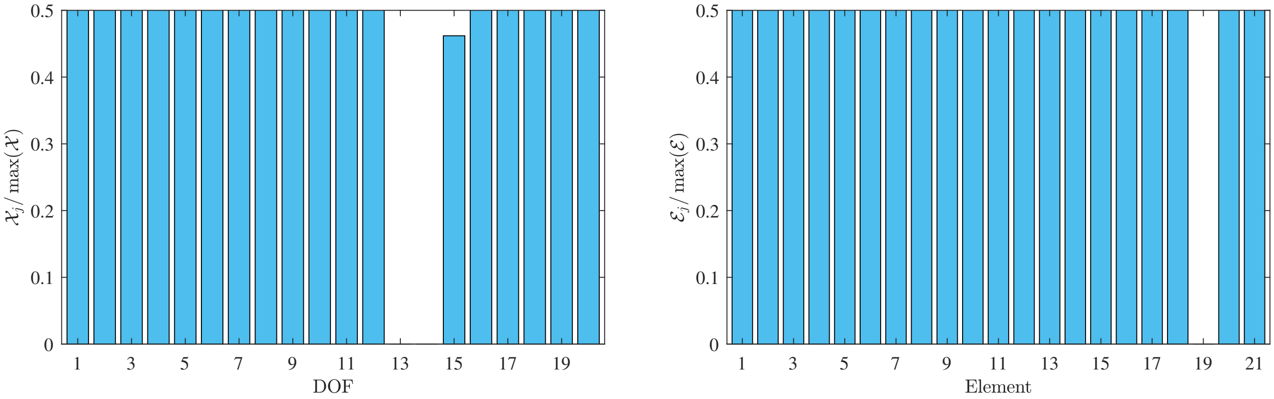

(a) **(b)**

Fig. 2: Damage localization of mass perturbation in node 9 (DOF 13 and 14) and stiffness perturbation in element 19 using the DDLV scheme; with aggregated steady-state (a) displacement and (b) strain fields.

5.1. *Example 1*

To verify the theoretical developments, we analyze the truss model in an idealized context without noise, modal truncation, or model errors. In the damaged state, a mass perturbation in node 9 (DOF 13 and 14) and a stiffness perturbation in element 19 are introduced. Since we operate in the idealized setting, the extents of the perturbations and the s-values at which the interrogation is conducted are immaterial. The localization results using the DDLV scheme are presented in Fig. 2, where Fig. 2a shows the aggregated steady-state displacements of the unconstrained nodes and Fig. 2b shows the aggregated steady-state strains in the elements. Evidently, both damage types are located correctly. Worth of explicit note is that, in agreement with the theoretical developments, the stiffness perturbation is not localizable through the displacement fields and the mass perturbation is not localizable through the strain fields.

5.2. *Example 2*

The truss model is now tested in an output-only simulation setting with a sampling frequency of 200 Hz and a sample length of 400,000. The system is subjected to broadband excitation and the output, which is captured in both DOF in each of nodes 2, 4, and 6, is taken as displacements contaminated with 5 % white Gaussian noise. Model errors are introduced such that the *simulation models*—which replace the physical structure in its two states—are assigned random perturbations to the stiffness of each element, while the *interrogation model* used to compute $\mathcal{G}(s)$ from (11) retains the nominal stiffness. The perturbations are drawn from a uniform distribution with lower and upper limits of 0.98 and 1.02. In the damaged state, a point mass corresponding to 1 % of the total mass of the truss is added to node 9. The state and output matrices from the two structural states are estimated using stochastic subspace identification (SSI) [24] with a fixed model order of $N = 12$ to comply with the constraint $N \leq 2m$ established in Subsection 3.1. The six first modes of the truss are consistently identified in both structural states and are therefore used in the damage localization analysis. In Table 1, the estimated eigenvalues of the six modes are presented along with the exact ones of the interrogation model.

Tb. 1: Estimated eigenvalues of the simulation models and exact eigenvalues of the nominal model.

Mode no.	Nominal model (exact)	Simulation models	
		Reference (estimated)	Damaged (estimated)
1	−0.2548 + 12.7358i	−0.2563 + 12.7363i	−0.2475 + 12.5059i
2	−0.5697 + 28.4816i	−0.5703 + 28.4904i	−0.5466 + 27.9212i
3	−0.6287 + 31.4295i	−0.6294 + 31.4502i	−0.6149 + 31.0525i
4	−0.8930 + 44.6393i	−0.8948 + 44.7003i	−0.8908 + 44.4694i
5	−1.2336 + 61.6693i	−1.2341 + 61.6758i	−1.1494 + 59.9382i
6	−1.2883 + 64.4008i	−1.2942 + 64.7070i	−1.2702 + 63.9391i

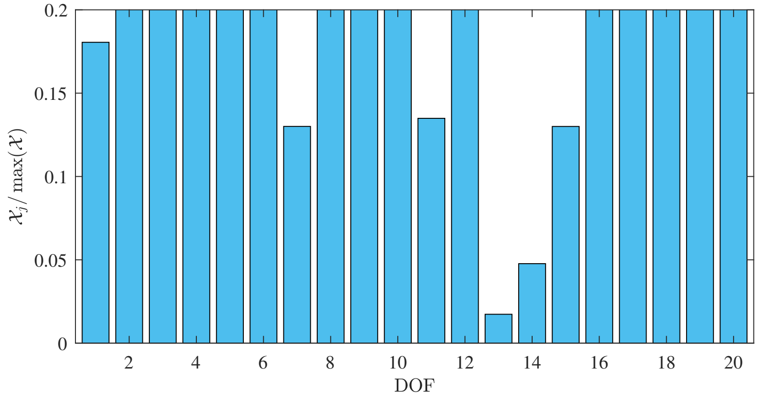

Fig. 3: Localization of mass perturbation in node 9 (DOF 13 and 14) using the SDDLV scheme.

The SDDLV scheme is implemented with four distinct s-values, namely, $s \in \{-0.2+10\mathrm{i}, -0.4+24\mathrm{i}, -0.7+35\mathrm{i}, -1+55\mathrm{i}\}$. By aggregating the steady-state displacements obtained for these s-values, the localization results shown in Fig. 3 are obtained for the unconstrained nodes. The two lowest aggregated displacement values are obtained for DOF 13 and 14, which are the DOF in node 9 (where the mass perturbation is added). The third lowest aggregated displacement value—being approximately three times larger than the value for DOF 14—is obtained for DOF 15, which is the horizontal DOF in node 10, see Fig. 1.

6. Experimental study

The applicability of DDLVs for locating mass perturbations is tested experimentally in the context of the steel frame depicted in Fig. 4a. The geometrical specifications of the frame are provided in Fig. 4b, and it is noted that the columns and floors are welded together. We analyze two structural states; namely, the reference and a "damaged" one in which a mass perturbation of 0.3 kg (constituting approximately 0.7 % of the frame's mass) is added to the second floor. In each experimental trial, the frame is subjected to a measured impulse load at the third floor that excites bending around the weak axis, and the response is captured with eight uniaxial accelerometers distributed as shown in Fig. 4b. Here, it is noted that accelerometer 2 is co-located with the input.

6.1. Data processing and DDLV extraction

The input transducer and the installed sensors sample with a frequency of 4,096 Hz for a duration of 16 s in each trial. Fig. 5a depicts a selected interval of the experimental frequency response functions based on the acceleration output captured in sensor 1 for the two structural states. This interval contains the first four bending modes of which the second and fourth exhibit notable sensitivity to the mass perturbation. The transfer matrix for each of the two structural states is computed by applying SSI to the measured temporal input-output realizations. The SSI is set up with a model order of 8, which results in consistent identification of the first four bending modes in both structural states. The estimated modal parameters are listed in Table 2, where it, in compliance with the frequency response functions in Fig. 5a, is seen how the second and fourth eigenvalues display notable sensitivity to the mass perturbation. It is noted that the mode shapes are evaluated by the modal assurance criterion (MAC) values [25] between "coinciding" modes (that is, the diagonal components in the MAC matrix).

The DDLV scheme is implemented with four distinct s-values, namely, $s_i = 0.9\lambda_i$, $i = 1, \ldots, 4$, where λ_i is the eigenvalue of the ith mode in the reference state. Fig. 5b shows the singular values of $\delta G(s)$, which do not suggest rank deficiency of $\delta G(s)$. The lack of rank deficiency is expected due to measurement noise, but, as will be evidenced in Subsection 6.3, the right singular vector associated with the smallest singular value may still possess information on the damage location.

6.2. Finite element model formulation

A two-dimensional finite element model of the frame is established by use of 26 two-dimensional Euler-Bernoulli beam elements; each with geometric specifications in accordance with the physical quantities presented introductory in the present section. The model, which is depicted in Fig. 4c, is classically damped with the damping ratios of the first four modes coinciding with the experimental findings, see Table 2. The mass density of the material model is set to 8,085 kg/m^3 to attain

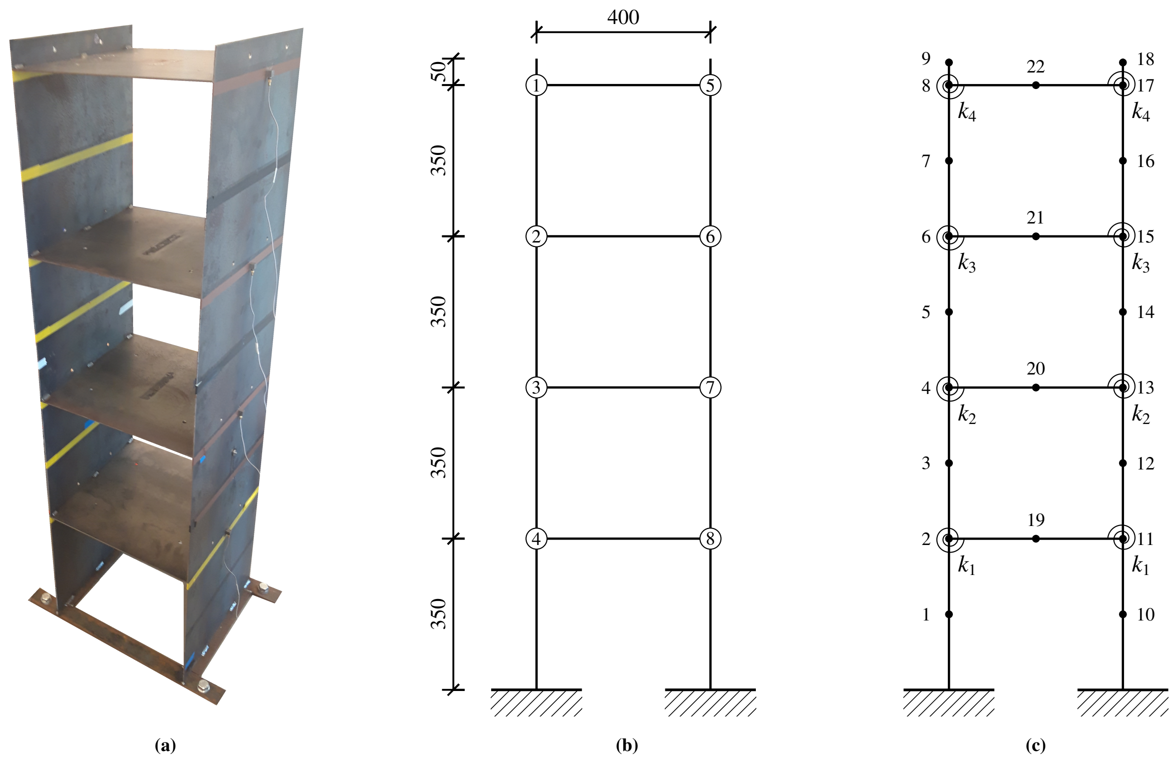

Fig. 4: Frame with (a) showing the reference state, (b) a sketch with accelerometer distribution and geometric dimensions in mm, and (c) a node-numbered finite element beam model representation with rotational springs (with stiffness k_i) in the joints. The input is co-located with accelerometer 2.

the mass of the real frame structure, and the modulus of elasticity is set to 210 GPa. Rotational springs are implemented in the model to allow for flexibility in the joints between the columns and floors. It is assumed that the stiffnesses associated with springs at a particular floor are identical, thus a total of four spring stiffnesses, k_i, are to be determined. This is done through sensitivity-based parameter estimation [26] with the eigenfrequencies of the first four modes and the associated MAC values as features. With reference to Fig. 4c, we find $k_1 = 8.34 \cdot 10^3$, $k_2 = 7.48 \cdot 10^3$, $k_3 = 5.62 \cdot 10^3$, $k_4 = 4.93 \cdot 10^3$ N/m, which result in a model with the modal parameters presented in Table 2.

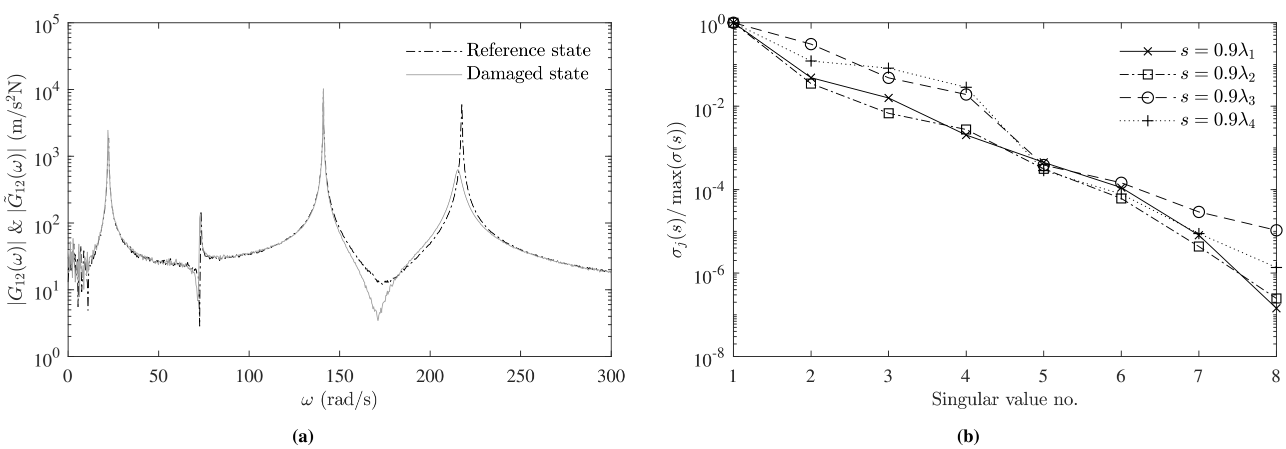

Fig. 5: Experimental realizations with (a) showing the frequency response functions (with output from sensor 1) from both structural states and (b) the singular values of $\delta G(s)$ for the selected s-values, where λ_i is the eigenvalue of the ith mode in the reference state.

Tb. 2: Estimated modal parameters of the frame in its reference (ref.) and damaged (dam.) states and model predictions[a] in the reference state.

Mode number	Eigenfrequencies (rad/s)			Damping ratios (%)		Diagonal MAC values	
	Model	Ref.	Dam.	Ref.	Dam.	Ref. – Dam	Ref. – Model
1	22.22	22.19	22.13	0.14	0.14	1.00	1.00
2	72.92	72.86	72.61	0.13	0.18	1.00	1.00
3	141.11	141.04	141.00	0.05	0.05	1.00	0.99
4	217.32	217.43	215.33	0.05	0.83	1.00	0.99

[a]The model is developed in Subsection 6.2. The damping ratios of the first four modes are taken as the experimental estimates in the reference state.

6.3. Damage localization results

The four DDLVs extracted in Subsection 6.1 are applied to the transfer matrix of the finite element model developed in Subsection 6.2 evaluated at the selected s-values. The resulting displacement fields (one per s-value) are aggregated in accordance with the implementation strategy outlined in Section 4, which provides the horizontal displacement components shown in Fig. 6. Since the mass perturbation is located in node 20, the DDLV method allows for localization of the perturbation through inspection of the aggregated horizontal displacement field. Specifically, the minimum aggregated horizontal displacement is in node 20; with a value that is approximately 1.5 times smaller than the second smallest value, which is attained in the adjacent node 4.

7. Conclusion

This paper shows that the DDLV and SDDLV schemes—originally presented as means of locating stiffness perturbations in structural systems—can also be used for mass perturbation localization. It is proved how application of DDLVs as structural loads will confine potential mass perturbations to the structural subdomain exhibiting zero steady-state motion, hence allowing for localization of mass perturbations directly from the displacement fields. Stiffness perturbations follow from an interrogation of the strain fields, which are obtained through a linear transformation of the displacement fields. Therefore, the DDLV and SDDLV schemes enable localization of both damage types without requiring any modification of the original formulations by Bernal [14, 15]. In the present paper, this is verified in the context of numerical examples with a finite element truss structure model and an experimental study with a frame structure.

References

[1] C. R. Farrar, K. Worden, Structural health monitoring: A machine learning perspective, 1st Edition, John Wiley & Sons, 2013.

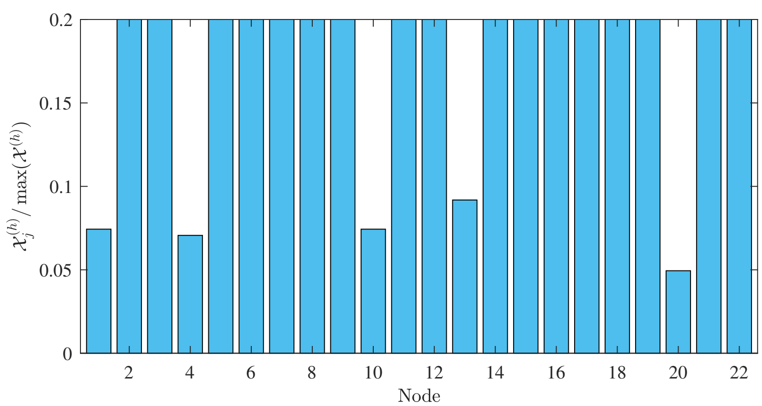

Fig. 6: Aggregated horizontal displacement components, $\mathcal{X}_j^{(h)}$, obtained using the DDLV method. The mass perturbation is located in node 20.

[2] M. D. Ulriksen, Damage localization for structural health monitoring: An exploration of three new vibration-based schemes, Doctoral dissertation, Aalborg University (2018).

[3] M. I. Friswell, Damage identification using inverse methods, Philosophical Transactions of the Royal Society A 365 (1851) (2007) 393–410. doi:10.1098/rsta.2006.1930.

[4] E. Reynders, A. Teughels, G. D. Roeck, Finite element model updating and structural damage identification using omax data, Mechanical Systems and Signal Processing 24 (5) (2010) 1306–1323, special Issue: Operational Modal Analysis. doi:10.1016/j.ymssp.2010.03.014.

[5] D. Bernal, M. D. Ulriksen, Output feedback in the design of eigenstructures for enhanced sensitivity, Mechanical Systems and Signal Processing 112 (2018) 22–30. doi:10.1016/j.ymssp.2018.04.032.

[6] T. W. Lim, T. A. L. Kashangaki, Structural damage detection of space truss structures using best achievable eigenvectors, AIAA Journal 32 (5) (1994) 1049–1057. doi:10.2514/3.12093.

[7] M. Basseville, L. Mevel, M. Goursat, Statistical model-based damage detection and localization: subspace-based residuals and damage-to-noise sensitivity ratios, Journal of Sound and Vibration 275 (3) (2004) 769–794. doi:10.1016/j.jsv.2003.07.016.

[8] D. Bernal, A. Kunwar, Steady state shift damage localization, Meccanica 51 (11) (2016) 2861–2871. doi:10.1007/s11012-016-0501-4.

[9] M. D. Ulriksen, D. Bernal, L. Damkilde, Shaped input distributions for structural damage localization, Mechanical Systems and Signal Processing 110 (2018) 499–508. doi:10.1016/j.ymssp.2018.03.039.

[10] S. Allahdadian, M. Döhler, C. Ventura, L. Mevel, Towards robust statistical damage localization via model-based sensitivity clustering, Mechanical Systems and Signal Processing 134 (2019) 106341. doi:10.1016/j.ymssp.2019.106341.

[11] D. Bernal, M. D. Ulriksen, Subspace exclusion zones for damage localization, Mechanical Systems and Signal Processing 114 (2019) 120–127. doi:10.1016/j.ymssp.2018.05.002.

[12] D. Bernal, Load vectors for damage localization, Journal of Engineering Mechanics 128 (1) (2002) 7–14. doi:10.1061/(ASCE)0733-9399(2002)128:1(7).

[13] D. Bernal, Flexibility-based damage localization from stochastic realization results, Journal of Engineering Mechanics 132 (6) (2006) 651–658. doi:10.1061/(ASCE)0733-9399(2006)132:6(651).

[14] D. Bernal, Damage localization from the null space of changes in the transfer matrix, AIAA Journal 45 (2) (2007) 374–381. doi:10.2514/1.25037.

[15] D. Bernal, Load vectors for damage location in systems identified from operational loads, Journal of Engineering Mechanics 136 (1) (2010) 31–39. doi:10.1061/(ASCE)EM.1943-7889.0000067.

[16] R. J. Johansen, L. M. Hansen, M. D. Ulriksen, D. Tcherniak, L. Damkilde, Damage localization in a residential-sized wind turbine blade by use of the SDDLV method, Journal of Physics: Conference Series 628 (2015) 012069. doi:10.1088/1742-6596/628/1/012069.

[17] M. D. Ulriksen, D. Tcherniak, L. M. Hansen, R. J. Johansen, L. Damkilde, L. Frøyd, In-situ damage localization for a wind turbine blade through outlier analysis of stochastic dynamic damage location vector-induced stress resultants, Structural Health Monitoring 16 (6) (2017) 745–761. doi:10.1177/1475921716681727.

[18] M. Döhler, L. Marin, D. Bernal, L. Mevel, Statistical decision making for damage localization with stochastic load vectors, Mechanical Systems and Signal Processing 39 (1) (2013) 426–440. doi:10.1016/j.ymssp.2012.12.011.

[19] L. H. G. Marin, M. Döhler, D. Bernal, L. Mevel, Robust statistical damage localization with stochastic load vectors, Structural Control and Health Monitoring 22 (3) (2015) 557–573. doi:10.1002/stc.1686.

[20] M. D. H. Bhuyan, G. Gautier, N. Le Touz, M. Döhler, F. Hille, J. Dumoulin, L. Mevel, Vibration-based damage localization with load vectors under temperature changes, Structural Control and Health Monitoring 26 (11) (2019) e2439. doi:10.1002/stc.2439.

[21] E. Reynders, R. Pintelon, G. D. Roeck, Uncertainty bounds on modal parameters obtained from stochastic subspace identification, Mechanical Systems and Signal Processing 22 (4) (2008) 948–969. doi:10.1016/j.ymssp.2007.10.009.

[22] G. Casella, R. L. Berger, Statistical Inference, 2nd Edition, Duxbury, 2002.

[23] G. H. Golub, C. F. Van Loan, Matrix Computations, 3rd Edition, The John Hopkins University Press, 1996.

[24] P. v. Overschee, B. De Moor, Subspace identification for linear systems: Theory - implementation - applications, 1st Edition, Kluwer Academic Publishers, 1996.

[25] R. J. Allemang, The modal assurance criterion (mac): Twenty years of use and abuse, Sound and Vibration 37 (8) (2003) 14–21.

[26] J. E. Mottershead, M. Link, M. I. Friswell, The sensitivity method in finite element model updating: A tutorial, Mechanical Systems and Signal Processing 25 (7) (2011) 2275–2296.